J. Hydrol. Hydromech., 69, 2021, 1, 29–40
DOI: 10.2478/johh-2020-0042
ISSN 1338-4333

©2021. This is an open access article distributed under the Creative Commons Attribution NonCommercial-NoDerivatives 4.0 License

sciendo Journal of Hydrology and Hydromechanics

The effects of rainfall characteristics and land use and cover change on runoff in the Yellow River basin, China

CaiHong Hu[1], Guang Ran[1], Gang Li[2], Yun Yu[3], Qiang Wu[1], Denghua Yan[1], Shengqi Jian[1*]

[1] College of Water Conservancy Science & Engineering, Zhengzhou University, No.100, Science Road, Zhengzhou, China.
[2] Jiangsu Province Luoyun Hydraulic Engineering Management Division, No.2, Huanghe Road, Xingfu street, Suqian City, China.
[3] China Machinery International Engineering Design & Research Institute CO., LTD, Zidong Creative Park, Qixia District, Nanjing, China.
[*] Corresponding author. Tel.: +86 18603814081. E-mail: jiansq@zzu.edu.cn

Abstract: The changes of runoff in the middle reaches of the Yellow River basin of China have received considerable attention owing to their sharply decline during recent decades. In this paper, the impacts of rainfall characteristics and land use and cover change on water yields in the Jingle sub-basin of the middle reaches of the Yellow River basin were investigated using a combination of statistical analysis and hydrological simulations. The Levenberg Marquardt and Analysis of Variance methods were used to construct multivariate, nonlinear, model equations between runoff coefficient and rainfall intensity and vegetation coverage. The land use changes from 1971 to 2017 were ascertained using transition matrix analysis. The impact of land use on water yields was estimated using the *M-EIES* hydrological model. The results show that the runoff during flood season (July to September) decreased significantly after 2000, whereas slightly decreasing trend was detected for precipitation. Furthermore, there were increase in short, intense, rainfall events after 2000 and this rainfall events were more conducive to flood generation. The "Grain for Green" project was carried out in 1999, and the land use in the middle reaches of the Yellow River improved significantly, which make the vegetation coverage (V_c) of the Jingle sub-basin increased by 13%. When V_c approaches 48%, the runoff coefficient decreased to the lowest, and the vegetation conditions have the greatest effect on reducing runoff. Both land use and climate can change the water yield in the basin, but for areas where land use has significantly improved, the impact of land use change on water yield plays a dominant role. The results acquired in this study provide a useful reference for water resources planning and soil and water conservation in the erodible areas of the middle reaches of the Yellow River basin.

Keywords: Land-use; Rainfall characteristics; Nonlinear model; *M-EIES* model; Yellow River.

1 INTRODUCTION

Water resources play an important role in life and have extremely important socio-economic significance in different sectors, such as agriculture, industry, trade, food production and hydropower generation (Wang et al., 2019; Zhan et al., 2014). However, in recent decades, due to over-exploitation and irrational use of water resources, water resources problems have become a major challenge, which threatened socio-economic development and ecological environment (Kong et al., 2016). The runoff in the Yellow River has been significantly reduced, with sudden changes occurring after the 1980s (Wang et al, 2013). Human activities (e.g., Grain for Green Project) and climate change (e.g., rainfall and temperature) are considered to be the key factors for the dramatic reductions in runoff in the middle reaches of the Yellow River (Liu et al., 2020; Xin et al., 2009). Climate variation will change the spatial-temporal distribution of global water resources, and underlying surface conditions change is one of the driving factors in the short term (Du et al., 2012; Oudin et al., 2018). In the background of population growth and increasing demands for important natural resources, focusing on the impact of underlying surface condition on the regional runoff generation mechanism is an urgent need for watershed management and hydrological disaster prevention.

The climate and underlying surface condition are the two dominant factors controlling flood formation. The impact of climate change on the runoff process mainly depends on the effect of rainfall and rainfall intensity on runoff generation. Many studies confirmed that the change of runoff in a watershed is affected by precipitation. If the underlying surface does not change, an increase in precipitation results in an increase in runoff (Asselman et al., 2003; Ou et al., 2018). However, the main factors controlling the environmental changes of flood formation are the variation of runoff generation and confluence conditions caused by changes in the underlying surface conditions. These changes are affected by human activities, such as destruction of forest vegetation, construction of hydraulic structures on rivers, large-scale irrigation and drainage, water and soil conservation measures, changes of land-use patterns, and urbanization and industrialization (Liu et al., 2017; Zhao et al., 2013a; Zuo et al., 2016). Variations in the underlying surface conditions caused by land-use are the primary reason for changes in surface water resources and flood occurrence under the same rainfall conditions (Gao et al., 2020; Zope et al., 2016).

Since the launch of the "Grain for Green" project (GGP) after 1999, the vegetation coverage in the Helong area of the middle reaches of the Yellow River has increased significantly. Vegetation is an important component of soil and water conservation and is a core aspect of ecological construction in the Yellow River basin. Vegetation is also one of the primary ways to improve the ecological environment of the Yellow River basin (Yang et al., 2018; Zhao et al., 2013b). In the past 50 years, China has successively implemented a series of ecological construction projects (Gao et al., 2011). Most of these major initiatives are focused on vegetation restoration and reconstruction and promote the development of the regional water cycle.

There are two methods used to improve soil erosion in the Yellow River basin through vegetation restoration: (1) increasing effective vegetation coverage to change the water circulation path, which prevents soil erosion; and (2) increasing soil water content and increasing vegetation productivity.

The Yellow River water yield showed a notable downward trend after the 1980s (Wang et al., 2015). The cause of this sharp decline has been a significant focus of academic debate. Yin et al. (2017) found that land-use change may lead to important changes in runoff generation processes and water storage. Feng et al. (2012) pointed out that large-scale vegetation restoration on the Yellow River basin was the main reason for the reduction of water yield. Zhao et al. (2013a), however, found that climate change accounted for more than 50% of the reduction in runoff in the middle reaches of the Yellow River. Although many researches have explored the reason of water and sediment changes in the middle reaches of the Yellow River from the perspective of climate and land use, it is still unclear how the significant increase in vegetation coverage caused by land use changes and different rainfall characteristics will affect the runoff process, and additional research is required, in particular, whether it has an impact on Catastrophic Rainstorm floods and standard flood of watershed planning.

After 2000, the most significant improvement in the vegetation cover occurred mainly in the gullied hilly areas of the middle reaches of Yellow River. Therefore, this study used the Jingle sub-basin in the middle reaches of the Yellow River as the study area. This paper analyzes the influence of rainfall characteristics and vegetation coverage on runoff process during flood season (July to September) and explores the nonlinear relationship between runoff and the factors that control runoff (precipitation, rainfall intensity, vegetation coverage, and antecedent precipitation index). Additionally, the runoff process under different underlying surface conditions is studied using a distributed hydrological model. The aims of the present study were to (1) investigate the impact of different rainfall characteristics and vegetation coverage on runoff process; (2) establish non-linear model of runoff coefficient based on rainfall characteristics and vegetation conditions; and (3) apply the *M-EIES* hydrological model to analyze the impact of land use and climate changes on water yield. The results obtained in this research can provide useful information for water resources planning and management as well as that for water and soil conservation in areas where the underlying surface conditions of the middle reaches of the Yellow River have improved significantly.

2 MATERIALS AND METHODS

2.1 Study area

The Fen River, located in the Shanxi province in northern China, is one of the largest tributaries of the Yellow River. The drainage area of the Fen River basin is 39,471 km^2. The river basin has a continental monsoon climate with monthly average temperatures ranging from 4°C to 13°C. The area has an average annual precipitation of 503 mm, 60% of which occurs between July and September. The average annual runoff of the basin is 57.76mm/year. The land in this area is predominantly used for forest and farmland, although the development of towns has increased with the fast pace of urbanization. The region of interest for this study is located in the north and upper reaches of the Fen River basin (Fig. 1).

The drainage area of the Jingle sub-basin is 2799 km^2. The main channel length is 83.9 km, the average slope of the main stream is 6.7%, and the shape coefficient of the basin is 0.398. The "Grain for Green" project began in 1999and has had a great impact on water resources and floods (Jian et al., 2019; Wang et al., 2018).

2.2 Data collection

2.2.1 Land-use data

We obtained the Landsat Thematic Mapper (TM) imagery of the years 1971, 1999, and 2017 from the Global Land Cover Facility. These images were used to show the variation of land-use in the experimental period (Fig. 2). The digital elevation model (DEM), with a spatial resolution of 30 m, was downloaded from the China Soil Scientific Database (CSSD). Soil type data of the Jingle sub-basin were taken from the Consultative Group on International Agricultural Research-Consortium for Spatial Information (CGIAR-CSI).

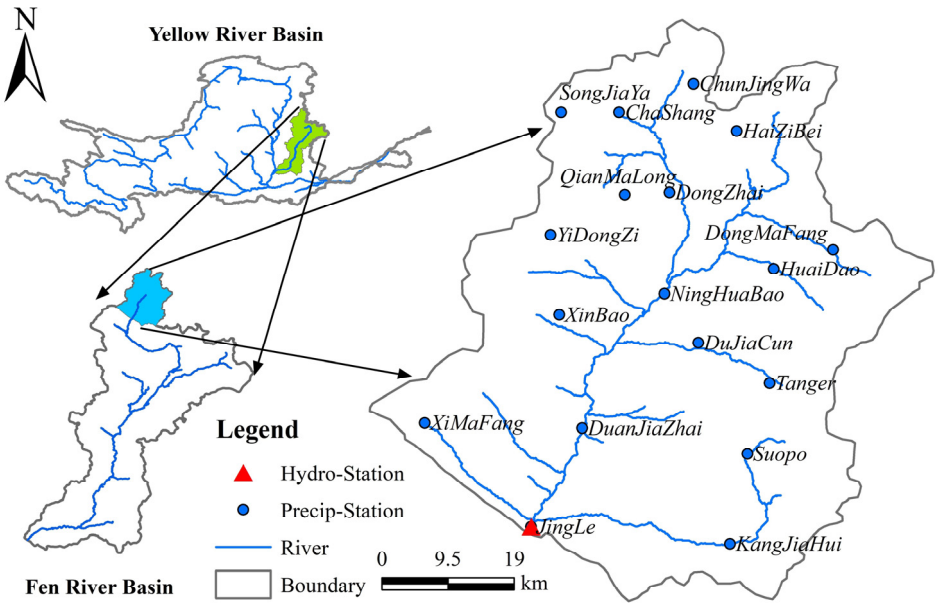


Fig. 1. Locations of the study area and gauging stations.

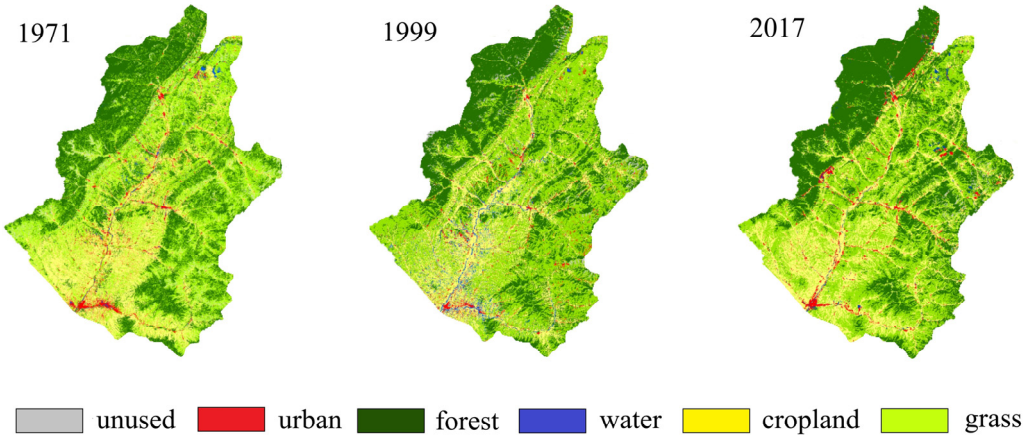


Fig. 2. Land-use types of Jingle sub-basin in 1971, 1999, and 2017.

Table 1. Land use transfer matrix from 1971 and 1999.

1971/1999	Farmland (km^2)	Forest (km^2)	Grass (km^2)	Water (km^2)	Urban (km^2)	Total (km^2)
Farmland (km^2)	679.41	13.52	64.95	0.02	0.22	758.12
Forest (km^2)	0.64	894.24	4.65	0.00	0.00	899.53
Grass (km^2)	3.90	88.30	996.14	0.12	0.09	1088.55
Water (km^2)	0.00	0.00	0.45	35.76	0.00	36.21
Urban (km^2)	0.03	0.16	0.34	0.00	16.05	16.58
Total (km^2)	683.98	996.23	1066.53	35.90	16.35	2799.00

Table 2. Land use transfer matrix from 1999 and 2017.

1999/2017	Farmland (km^2)	Forest (km^2)	Grass (km^2)	Water (km^2)	Urban (km^2)	Total (km^2)
Farmland (km^2)	568.99	13.55	100.95	0.23	0.04	683.77
Forest (km^2)	0.91	987.02	8.38	0.00	0.14	996.45
Grass (km^2)	4.71	61.57	999.69	0.37	0.18	1066.52
Water (km^2)	0.05	0.10	0.12	35.64	0.00	35.91
Urban (km^2)	0.00	0.11	0.25	0.00	16.01	16.36
Total (km^2)	554.46	1072.15	1119.78	36.19	16.42	2799.00

Table 1 and Table 2 show the detailed information of the land-use change. From 1971 to 1999, the areas of farmland and grassland decreased by 74.14 and 22.02 km^2, respectively, while the forested area increased by 96.7 km^2. This increase was caused by the conversion from grassland and cultivated land to forest. From 1999 to 2017, the areas occupied by farmland, grassland, and forest decreased by 129.31 km^2, increased by 53.26 km^2, and increased by 75.7 km^2, respectively. These changes in area exemplify the conversion from farmland to grassland and from grassland and farmland to forest. Water areas and urban construction show little change.

2.2.2 Vegetation coverage data

The Normalized Difference Vegetation Index (*NDVI*) data for 1971–1981 were extracted using ENVI Version 5.3. We used these data to perform radiometric calibration and atmospheric correction on Landsat TM (1971–1980, spatial resolution 30 m × 30 m) remote sensing images. The *NDVI* data for 1981–2017 were obtained from the GIMMS *NDVI* dataset, which is a

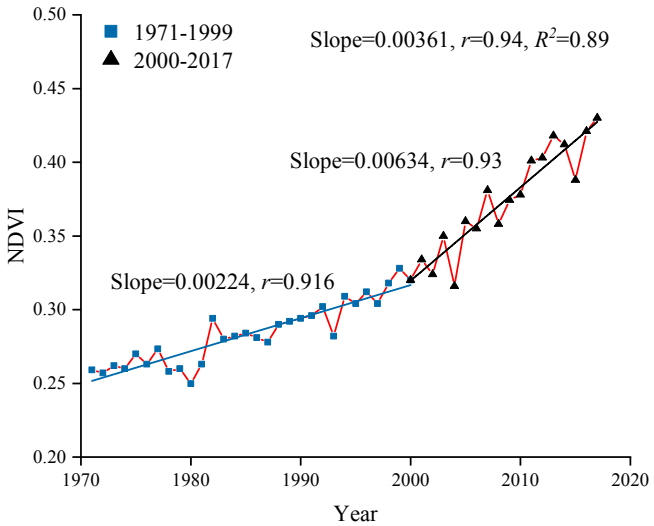


Fig. 3. The mean monthly *NDVI* of flood season between 1971 and 2017.

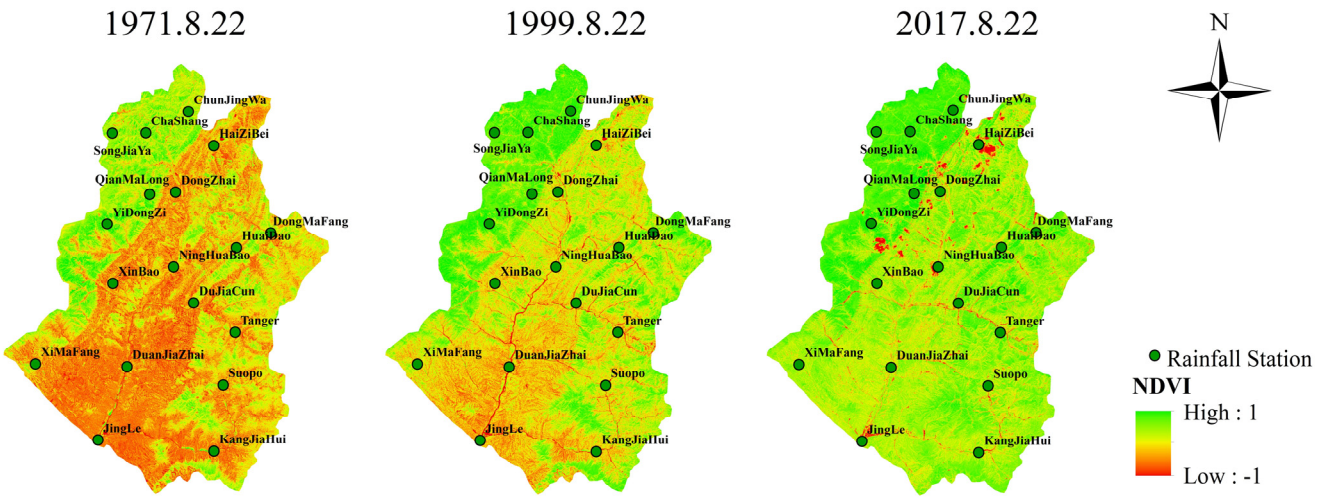


Fig. 4. The distribution of *NDVI* in the August 22nd of 1971, 1999, and 2017.

semi-monthly composite with 250 m resolution. Land-use was classified according to the *NDVI* data of the watershed and the CART decision tree method. Then, the thresholds of 5% and 95% of forest and grassland were taken as the minimum and maximum values of *NDVI*. Finally, the *NDVI* maximum and minimum and the dimidiate pixel model (DPM) are used to invert the vegetation coverage data.

The mean monthly *NDVI* for flood seasons shows an increasing trend in vegetation coverage in the Jingle sub-basin from 1971 to 2017. Two periods were considered in this study 1971–1999 and 2000–2017, and the average values of *NDVI* in the two periods were 0.283 and 0.374, with a growth rate of up to 32%, as shown in Fig. 3. Figure 4 shows the distribution of *NDVI* on August 22nd of 1971, 1999, and 2017. Vegetation restoration is most obvious in the central and southern parts of the basin.

2.2.3 Hydro-meteorological data

The hydrological data included precipitation, evaporation, and runoff from 1971 to 2017. There are 16 hydrological stations in the Jingle sub-basin of the Fen River basin (Fig. 1). Hydrological stations were extracted from a database of the minstry of the Yellow River Conservancy Commission, which is publicly available at www.yrcc.gon.cn under the Data of the Yellow River basin section. And the hourly rainfall and evaporation data were employed for *M-EIES* hydrological modeling.

2.3 Methods

2.3.1 Rainfall and runoff

We calculated area-averaged rainfall using the Thiessen polygon method. Rainfall duration was an effective duration and did not take intermittent time into account (Cuevas et al., 2019). The average rainfall intensity was calculated by taking the ratio of surface rainfall to rainfall duration, and the runoff coefficient (α) was calculated by taking the ratio of precipitation (P) to runoff (R). We used the storage-discharge relationship method (Ajami et al., 2011) to calculate the runoff depth R:

$$R = \frac{3.6\Delta t\left[\sum_{i=2}^{n-1} Q_i + \frac{Q_1 + Q_n}{2} + (Q_n - Q_1)K\right]}{A} \quad (1)$$

$$\alpha = \frac{R}{P} \quad (2)$$

where Δt is the period length (h); Q_i is the i-period flow (m^3/s); n is the number of periods; A is the basin area (km^2); and K is the storage coefficient.

2.3.2 Antecedent precipitation index

The antecedent precipitation index (*API*) reaction is defined as the amount of rainfall retained in the soil after a rain event. In this study, we used the recursive formula method (Walhin, 2000) to estimate the accumulation of rainfall in the soil at the early stages of the flood development. The *API* is defined mathematically as follows:

$$API_t = kP_{t-1} + k^2P_{t-2} + \ldots + k^n(API_{t-n} + P_{t-n}) \quad (3)$$

where API_t is the antecedent precipitation index (mm) on day t; API_{t+1} is the antecedent precipitation index (mm) on $t + 1$ day; n is the number of previous rain days affecting the runoff (usually ~15 days); P_t is the t-day rainfall (mm); P_{t-1}, P_{t-2}… is the rainfall (mm) 1 day before t day, 2 days before…; and k is the daily regression coefficient of the soil water content, defined as follows:

$$k = 1 - \frac{E_m}{W_m} \quad (4)$$

E_m is the watershed evapotranspiration capacity (mm), and W_m is the water storage capacity (mm) of the watershed. Because E_m varies with region, season, rain and other conditions, k value is generally calculated according to the corresponding monthly average value of sunny day and rainy day or by month.

2.3.3 Water storage capacity

The watershed water storage capacity (W_m) is derived from multiple flood events (Hu et al., 2016), which selects the rainfall floods that can make the water content of the basin saturated and generate a large flood process. Then let $W_{m,0} = I_m$, where the loss $I_m = P - R$. The calculation process of W_m can be estimated as:

$$K_j = 1 - \frac{E_m}{W_{m,j}} \tag{5}$$

$$W_{0,j} = \sum_{0}^{n} P_d \times K_j^d \tag{6}$$

$$W_{m,j} = W_{m,j-1} + W_{0,j-1} \tag{7}$$

where K_j is the daily regression coefficient of soil water content under different iterations; P_d represents the rainfall for the d day before the flood; d is the power; j is the number of iterations; and $W_{m,0}$ is the assumed value for the first iteration. After multiple iterations, W_m approaches a fixed value, which represents the water storage capacity of the basin.

2.3.4 Data analysis

A multiple nonlinear regression analysis was performed to simulate the runoff coefficient. Four factors were used to estimate the coefficient: rainfall (P), rainfall intensity (i), vegetation coverage (V_c), and the antecedent precipitation index (API). For our regression analysis, the dependent variable (runoff coefficient) is defined by several independent variables (P, I, V_c, and API) as well as nonlinear combinations of the independent variables. We evaluated data using SPSS 16.0 for Windows (SPSS Inc., Chicago, IL, USA). To find the relationship between the independent and dependent variables, a nonlinear regression analysis is performed using the Levenberg-Marquardt method.

We used one-way analysis of variance (ANOVA) to assess the relationship between runoff and impact factors. The coefficient of determination (R^2), the sum of the squared errors (SSE), and the mean square error (MSE) are used to determine the quality of the regression. An R^2 close to 1 and an MSE smaller than 10% generally indicate an accurate prediction (Lewis, 1982; Nau, 2017):

$$R = \frac{n\sum y_i \hat{y}_i - (\sum y_i)(\sum \hat{y}_i)}{\sqrt{n\left(\sum y_i^2\right) - (\sum y_i)^2}\sqrt{n\left(\sum \hat{y}_i^2\right) - (\sum \hat{y}_i)^2}} \tag{8}$$

$$e_i = y_i - \hat{y}_i \tag{9}$$

$$MSE = \frac{1}{n}\sum_{i=1}^{m} e_i^2 \tag{10}$$

where R is correlation; R^2 is coefficient of determination $\hat{y}_i$ is the value of the dependent variable predicted by the model; y_i is the true value of the dependent variable; n is the number of samples; e_i is the residual.

2.3.5 *M-EIES* model

The Modified Excess Infiltration and Excess Storage (*M-EIES*) model was based on the Xinanjiang model (Zhao, 1992). Compared with the Xinanjiang model, the *M-EIES* model can organically combine the excess infiltration runoff mode with the storage runoff mode, which uses the characteristics of runoff in the middle reaches of the Yellow River. Furthermore, different infiltration and evaporation parameterizations are applied in the *M-EIES* model. A schematic diagram for *M-EIES* model is shown in Fig. 5. The *M-EIES* model has 24 parameters, 8 more than the Xinanjiang model. These new parameters reflect the different infiltration and evaporation rates under different land use conditions. A list of these parameters is presented in Table 3. In previous studies, this model has been used to simulate runoff at different stages in the Jingle sub-basin, and the changes in parameters of model at different stages have been discussed and studied (Wen et al., 2020).

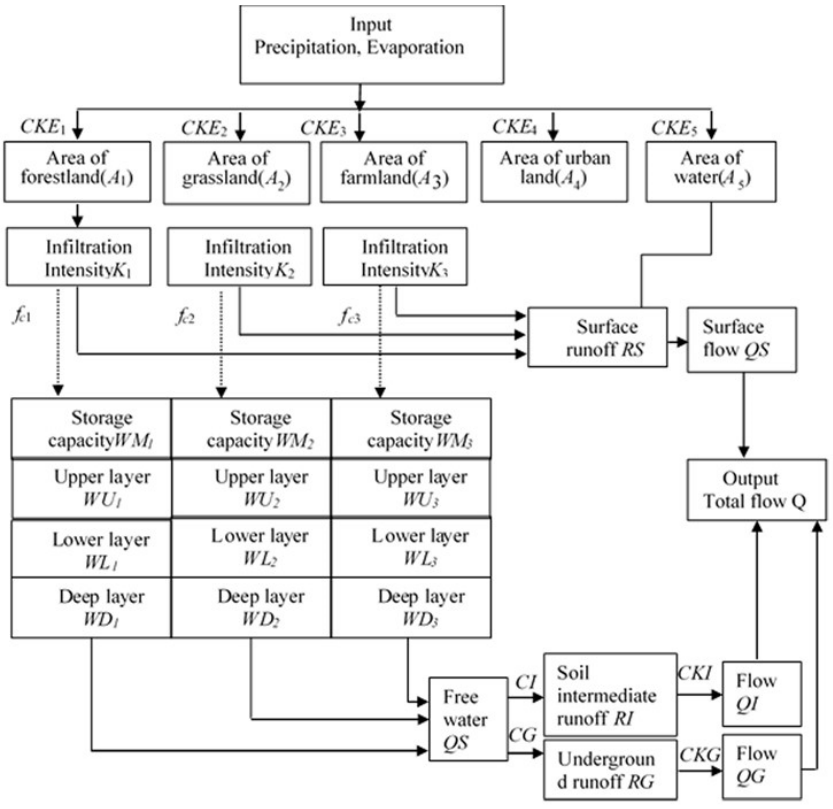


Fig. 5. Structure of *M-EIES* model.

Table 3. The meaning of the new parameters in *M-EIES* model.

New parameters	Parameter meaning	Range
CKE1	Forest land evaporation coversion	0.5–2
CKE2	Grass land evaporation coversion	0.5–2
CKE3	Urban land evaporation coversion	0.5–2
CKE4	Water evaporation coversion	0.5–2
fc1	Forest steady infiltration rate	4–6
fc2	Grass steady infiltration rate	4–6
fc3	Urban steady infiltration rate	4–6
fc4	Water steady infiltration rate	4–6

To analyze the impact of land-use changes on runoff generating processes, we built the *M-EIES* model based on land-use. Combined with the time point of GGP in the middle reaches of Yellow River, this study was divided into two periods: 1971–1999 and 2000–2017 (Xin et al., 2009). Land-use maps in 1985 and 2010 were used to represent the land-use patterns for the two periods. The following three scenarios were simulated:
Scenario1 (S1): climate during 1971–1999 and land use in 1985.
Scenario2 (S2): climate during 1971–1999 and land use in 2010.
Scenario3 (S3): climate during 2000–2017 and land use in 2010.

S1 reflects actual conditions during 1971–1999; S2 indicates how land use changes affected runoff, while S3 describes the combined effects of land use and climate changes on runoff.

In this study, we use *SCE-UA*, which combines the advantages of the simplex procedure with (1) controlled random search; (2) competitive evolution; and (3) complex shuffling (Duan et al., 1992), to solve model parameters. The initial values of the model parameters are given, and then the *SCE-UA* was run to obtain the approximate, optimal values of the model parameters. Additionally, we use the Nash-Sutcliffe efficiency coefficient (*NSE*), the coefficient of determination (R^2), and the relative error (R_e), to evaluate the validity of the model.

3 RESULTS AND DISCUSSION

3.1 Changes characteristic analysis of rainfall and runoff

3.1.1 Changes trends of rainfall and runoff

The changes in rainfall and runoff of 80 flood events for the Jingle sub-basin during the flood seasons (July to September) from 1971 to 2017 are shown in Fig. 6. The amount of runoff ranged from 1.01mm in 1986 to 26.13mm in 1982. These two flood events also were generated by the least (6.8 mm) and most (125 mm) rainfall, respectively. The 50 floods from 1971 to 2000 exhibit a similar fluctuation pattern between rainfall and runoff, the change in precipitation affected runoff change. However, after 2000, flood events with more rainfall were not necessarily associated with more runoff, these two parameters obviously lack synchronization. Overall, the rainfall duration tends to decrease with time, while the rainfall intensity remains stable.

Table 4 calculates the changes in the average values of hydro-meteorological variables for the two periods. The precipitation and rainfall duration decreased by 6.4% and 6.7%, and the rainfall intensity and maximum rainfall intensity increased by 22% and 37.8%, respectively, between the first (1971–1999) and the second (2000–2017) periods. Additionally, the runoff in the second period decreased by 28%, and the runoff coefficient decreased by 25.8%. The results show that the change of rainfall in the second stage is quite different from the change of corresponding runoff. This may be a result of soil and water conservation measures, such as converting farmland to forest or grass, or the construction of check dams (Li et al., 2014).

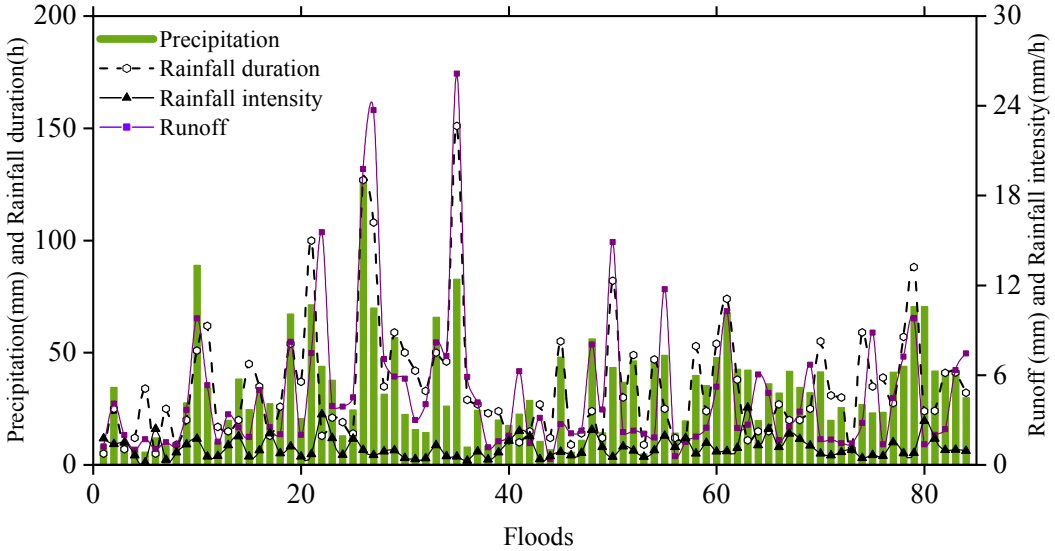


Fig. 6. The characteristics of variation of runoff, precipitation, rainfall intensity, and duration.

Table 4. Changes in average values of the hydrological characteristic value.

Hydro-meteorological charcateristic value	Period: I 1971–1999	Period: II 2000–2017	Change	Change rate
Precipitation(mm)	35.07	32.95	2.12	–6.40%
Rainfall intensity(mm/h)	1.08	1.32	0.24	22%
Maximum rainfall intensity(mm/h)	19	26.2	7.2	37.80%
Rainfall duration(h)	35.08	32.73	–2.35	–6.70%
Peak discharge(m^3/h)	376.4	256	–120.4	–31.90%
Runoff(mm)	5.29	3.8	–1.49	–28%
Runoff coefficient	0.17	0.126	–0.044	–25.80%

Table 5. The classification of rainfall types in two periods.

Rainfall types	Judgment criteria			Proportion of different stages	
	i (mm/h)	t (h)	i_{max} (mm/h)	1971–1999	2000–2017
I	>1.3	t < 20	i_{max} > 25	14 (28%)	13 (38%)
II	0.7 < i < 1.3	20 < t < 36	13 < i_{max} <25	26 (52%)	15 (44%)
III	< 0.7	t > 36	i_{max} < 13	10 (20%)	6 (18%)

3.1.2 Changes characteristic analysis of rainfall events

The temporal rainfall pattern refers to the distribution of precipitation with time. This distribution of precipitation has an important influence on infiltration, runoff generation, and soil erosion. Many scholars use different methods to analyze the rainfall patterns in different regions (Huff., 1967; Jeffrey and Eyal, 2003). Based on current research regarding the variations of rainfall characteristics for watersheds in China (Yin et al., 2014), and combined with the climatic conditions of Jingle subbasin, this study classifies 84 rainfall events into three types using rainfall intensity, rainfall duration, and maximum rainfall intensity (Table 5): shorter duration and higher intensity (type I), evenly-distributed (type II), and longer duration and lower intensity (type III). Type II was the most frequent type of rainfall events and accounted for 52% and 44% of the total rain events for the two periods. Compared with the first period, the proportion of type II and type III in 2000–2017 decreased by 8% and 2% respectively, while that of type I rainfall increased significantly.

3.2 Effect of rainfall and V_c on runoff

Figure 7 shows the effect of different types of rainfall on runoff. There were 16 flood events generated by rainfall events of type III; 41 floods generated by rainfall events of type II, and 27 floods generated by rainfall events of type I. When precipitation < 25 mm, runoff generated by three different types of rainfall has little change, and when precipitation > 25 mm, the type I rainfall events will generate more runoff as the continuous increase of rainfall. The results showed that precipitation was positively correlated with runoff, but under the same precipitation, the runoff pattern under different types of rainfall were more complicated, the rainfall events with shorter duration and higher intensity were more conducive to runoff generation, it was easier to cause water and soil erosion in the erosion area, which was the key point of water and soil loss prevention. Yang et al. (2019b) and Mu et al. (2015) found similar conclusion in other hilly area of the middle reaches of Yellow River in China.

The increase of forest and grassland has obviously increased the vegetation coverage after 2000. Therefore, it was necessary to study the impact of vegetation coverage on the runoff process. The runoff under different vegetation coverage was shown in the Figure 8. From 1971 to 1999 (before the "Grain for Green" project), the range of vegetation coverage in Jingle subbasin was 35%–45%, with an annual average growth rate of 0.36%. From 2000 to 2017, the range of vegetation coverage was 45%–58%, with an annual average growth rate of 0.76%. Under the same rainfall conditions, the runoff decreased as the vegetation coverage increased, and the runoff generated by unit rainfall decreases from 0.13 mm to 0.09 mm.

However, after 2000, the rainfall and runoff in Jingle subbasin lacked any synchronization (Fig. 6). The decrease in precipitation volume was an important factor leading to the decrease of runoff, but vegetation coverage restoration and

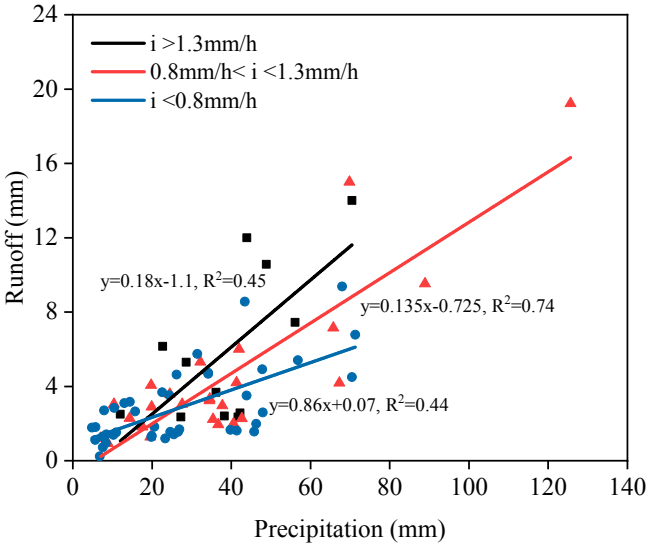


Fig. 7. The runoff generation process under different rainfall patterns.

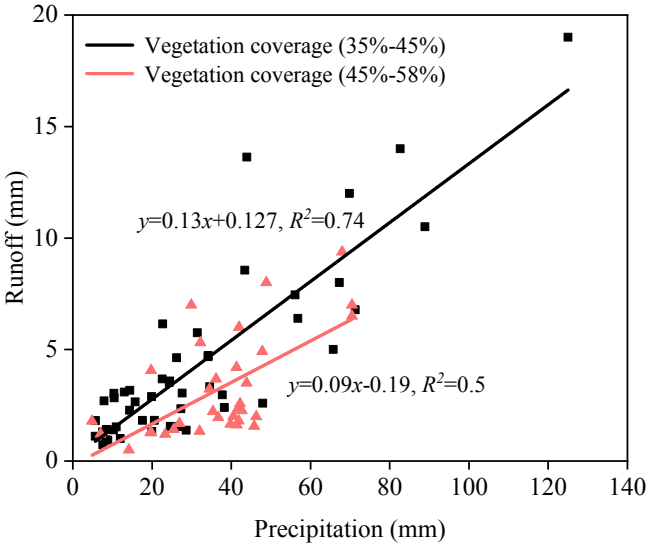


Fig. 8. The runoff generation process under different vegetation coverage.

improvement might also play a significant role, which could have ameliorated the decrease in annual runoff and sediment discharge by enhancing evapotranspiration (ET) and alleviating soil erosion (Hu et al., 2020; Yang et al., 2019a). With the development of soil and water conservation measures, evapotranspiration will increase and runoff will decrease (Wang et al., 2005; Xu, 2005). Over the past 20 years, the vegetation coverage in the regions of the Helong section had notable increased with the development of the GGP, which must have enhanced the intensity of evapotranspiration with a subsequent decrease in runoff. Meanwhile, vegetation can also affect infiltration by changing the hydraulic properties of the surrounding

soil (Minea et al., 2019). Most studies found that the growth and development of plant roots increased soil hydraulic conductivity from bare soil interspace to under canopy and improved the permeability of the soil (Bhark and Small, 2003; Chen et al., 2013). Thus, water and soil conservation measures to improve vegetation conditions, such as converting farmland to forest or grass, play an important role in reducing runoff. The significant increase in vegetation coverage may explain the decrease of runoff in the Helong section of the Yellow River.

3.3 Effect of rainfall and V_c on runoff coefficient

Runoff coefficient is an important parameter describing the relationship between rainfall and runoff, reflecting the runoff generation capacity of the basin (Chen et al., 2020). The rainfall intensity (i) and vegetation coverage (V_c) are the main factors used to determine the change of the runoff coefficient (Fig. 9). The runoff coefficient (α) shows a non-linear, decreasing trend with the increase of precipitation (P), rainfall intensity (i), and vegetation coverage. The rate of change of α is largest when V_c is ~35%–45%. As V_c continues to increase, α approaches to 0.064. There is a positive, nonlinear relationship between the antecedent precipitation index and the runoff coefficient, the fitting equation reaches a significant level, and the correlation coefficient is 0.75.

The runoff coefficient has an exponential relationship with rainfall intensity and a power function relationship with V_c and API. In this paper, the nonlinear relationship between α and its influencing factors is constructed using a multiple nonlinear regression method. The model parameters are determined using 50 rainfall and flood events within the Jingle sub-basin, and 34 rainfall and flood events are used to test the quality of the model. The original data were extremized to the interval (0,1) to reduce the error caused by decreasing the dimensions and the difference in magnitude of the impact factors. The Marquardt method and global optimization algorithm are employed to solve the parameters in the model. The runoff coefficient multivariate, nonlinear, regression model expression is given as:

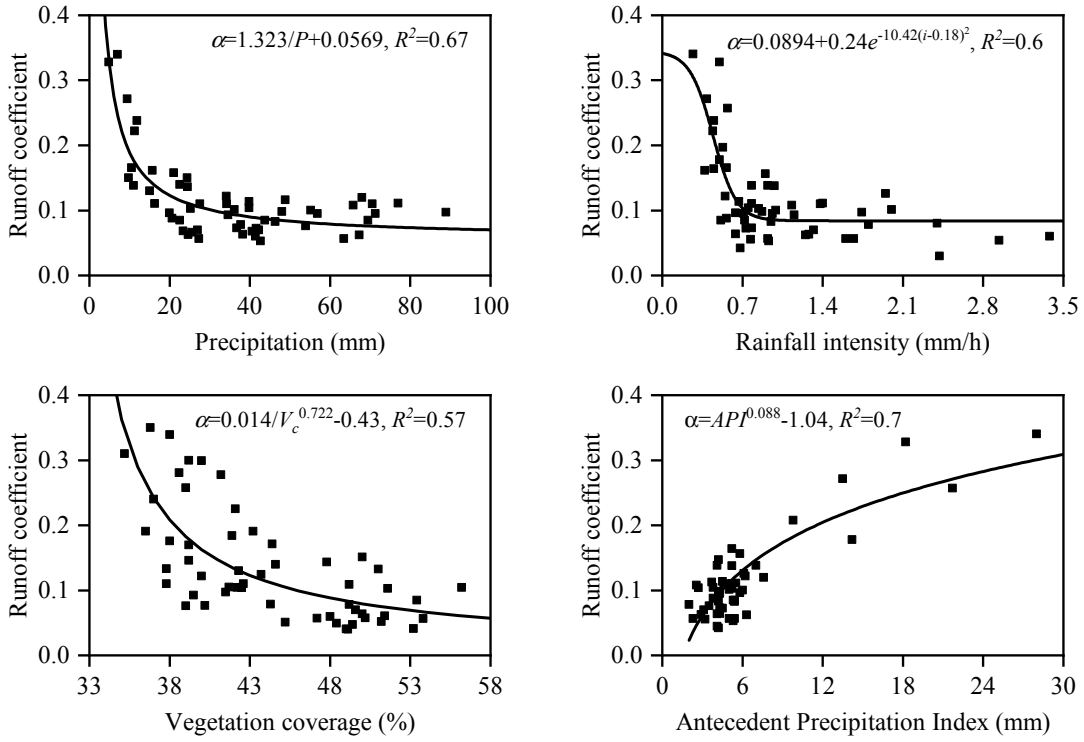


Fig. 9. The correlation between runoff coefficient and influencing factors.

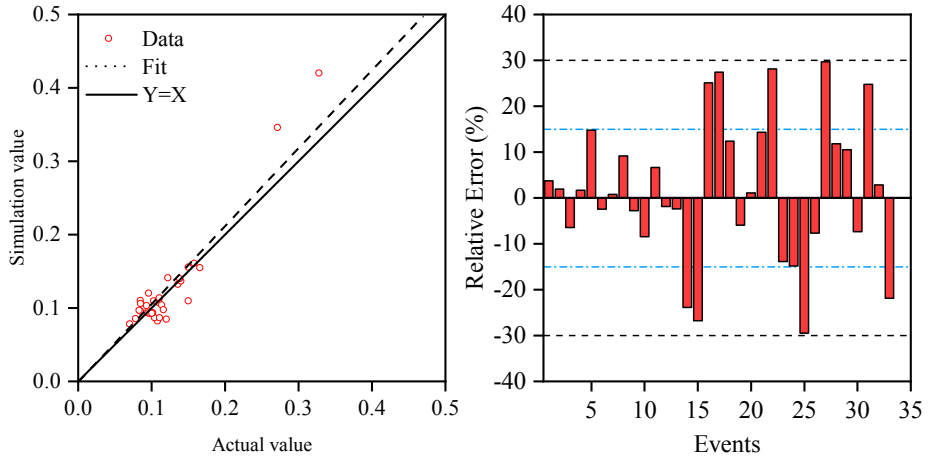


Fig. 10. Multivariate nonlinear model test of runoff coefficient.

$$\alpha = -0.205 + \frac{0.532}{P} + 0.055e^{(-0.5*\left[\frac{i-0.18}{0.219}\right]^2)} + \frac{0.001}{V_c^{0.722} - 0.55} + 0.25API^{0.067},$$

where α is the runoff coefficient (mm/mm); P represents precipitation (mm); i stands for rainfall intensity (mm/h); V_c means vegetation coverage (%); and API refers to antecedent precipitation index.

The model-generated coefficient of determination (R^2) was 0.841, which indicates that the regression model had statistical significance. The remaining data were used to test the fitting equation of α. The test results reported that the absolute value of the relative error of the test data did not exceed 30%. The relative error of 73% of the test data was within ±15%, which confirms the validity of the model (Fig. 10).

Analyzing the multivariate nonlinear regression equation, when the V_c and API of the Jingle sub-basin maintain a stable value, the runoff coefficient of the shorter duration and higher intensity rainfall events (Type I) is greater than Type II and Type III. Mu et al. (2015) found that for the same magnitude of rainfall, the overland flow and cumulative runoff increased with rainfall intensity in north semi-arid region of China. There is a threshold in the relationship between vegetation cover and soil erosion, and the impact of reducing runoff and soil erosion will become more obvious only when the density of V_c breaks through the threshold, which is about 30% in the Loess Plateau (Ludwig et al., 2005). The V_c of the Jingle sub-basin had increased from 40% to 53% during 1999–2007 period, breaking through the threshold of 30%. When V_c approaches 48%, the runoff coefficient decreased to the lowest, and the vegetation conditions have the greatest effect on reducing runoff. The Hydrological effects may significantly promote the reductions in runoff. And the significant increase in vegetation coverage may be an important driving force in explaining the sharp decrease in runoff along the middle reaches of the Yellow River.

3.4 Combined effect of climate changes and land use on runoff

Figure 11 shows the simulation results of runoff during the calibration (2000–2012) and validation (2013–2017) periods for the Jingle sub-basin. The evaluation indices, including the Nash-Sutcliffe efficiency (*NSE*), the coefficient of determination (R^2), and the relative error (R_e), are listed in Table 6. During the period of 2000–2017, we selected 8 flood events (5 flood events for model calibration and 3 flood events for model validation) with flood peaks ranging from 60 to 430 m^3/s. *NSE* of all the floods were greater than 0.7; R^2 were greater than 0.8, and R_e were smaller than 15%. The model parameters in the period of 2000–2017 was presented in Table 7. The above analyses indicate that the *M-EIES* model performed well in Jingle sub-basin. The following sections will use *M-EIES* model to simulate runoff with different land-use periods.

Table 8 shows the average water yield and peak flow simulated by the *M-EIES* model under different land-use conditions. The difference of water yield between S2 and S1, which indicates the effect of land-use change, showed a decrease of 1.93 mm, occupying 36.5% of the water yield under S1. The land-use changes under S2 decreased the peak flow by 139.4 m^3/s, which is 37% of the peak flow under S1. The difference in water yield between S3 and S1 represents the combined effects of land use and climate, showing a decrease of 1.87 mm and 132 m^3/s, which was 35.4% and 35.9% of the water yield and peak flow respectively. These results show that the land-use changes decreased the water yield in the Jingle sub-basin and reduced the peak flow in runoff.

Table 6. Evaluation indices for assessing the performance of runoff simulations.

Stage		Flood time	*NSE*	R^2	R_e(%)	Duration (h)
2000–2017	Calibration	20010711	0.75	0.84	13.5	38
		20010824	0.81	0.82	9.3	81
		20020811	0.85	0.82	8.5	100
		20030729	0.91	0.83	10.3	175
		20120726	0.87	0.87	9.1	115
	Validation	20130715	0.78	0.77	14.6	180
		20150801	0.82	0.84	9.5	68
		20160814	0.83	0.82	9.4	78

Table 7. The *M-EIES* model parameters in the period of 2000–2017.

Model parameters	Initialization parameter	Actual parameters	Model parameters	Initialization parameter	Actual parameter
WM	150	156.36	CKE3	1	1.423
X	0.2	0.283	f_{c1}	3.8	4.89
Y	0.3	0.296	K2	0.5	0.441
n	0.1	0.365	EX	3	2.67
m	0.1	0.169	SM	12	16.08
C	0.1	0.318	CKG	0.8	0.99
CKE1	1	1.104	CKI	0.8	0.999
f_{c1}	4.5	5.231	CI'	0.5	0.37
K1	0.5	0.348	CG	0.3	0.203
CKE2	1	0.985	N	3	3.505
fc2	4	5.024	NK	2.5	1.892
K2	0.5	0.415			

Table 8. Areal average water yield under different scenarios.

Scenarios	Land use	Climate	Water yield			Peak flow		
			Average (mm)	Change (mm)	Percent (%)	Average (m^3/s)	Change (m^3/s)	Percent (%)
1	1985	1971–1999	5.29	–	–	376	–	–
2	2010	1971–1999	3.36	1.93	36.5%	236.6	139.4	37%
3	2010	2000–2017	3.42	1.87	35.4%	241	135	35.9%

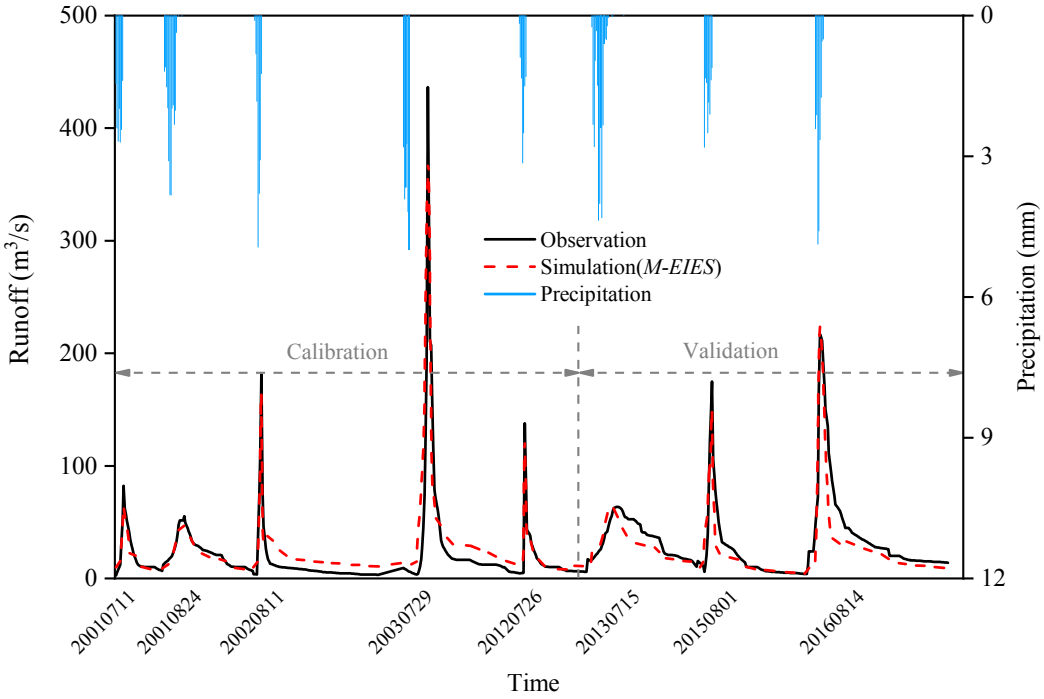


Fig. 11. Simulation results of Jingle sub-basin from 2000 to 2017 (The time step is 1 hour).

However, due to the interaction between land use change and climate change, the combined impact on water yield were almost equal to land use change. This phenomenon shows that for areas where land use has significantly improved, the impact of climate change on water yield is not obvious when the effect of land use change plays a dominant role.

The main cause of soil erosion in the middle reaches of the Yellow River was deforestation for land reclamation and cultivation on steep slopes. Grass have soil-consolidation ability due to its dense root system, whereas large-scale of farming on steep slopes will cause soil fertility decline and soil erosion (Li et al., 2014; Yue et al., 2014). In order to improve the underlying surface conditions of the basin, a series of soil and water conservation measures have been carried out in the middle reaches of Yellow River, like convert farmland to forest and grassland. Vegetation cover restoration and improvement can effectively reduce the water yield and improve the soil conservation of basins by delaying runoff, increasing infiltration and strengthening soil consolidation, which will avoid soil erosion and flood disasters (Wang et al., 2008). The control rate of soil and water conservation in the Jingle sub-basin was 6.8% before the 1970s, 27.1% in 1999, and 38.2% in 2010 (Ran et al., 2012). The significant increase in forest and grassland in the Jingle sub-basin and the decrease in farmland were the important factors for the decrease in water yield in that area. Therefore, the water and soil conservation measures and the GGP measures implemented in the 1990s have been effective on water yield reduction, which further confirms the rationality of the results of this study.

4 CONCLUSIONS

In this study, the impacts of rainfall characteristics on runoff in the Jingle sub-basin of the middle reaches of Yellow River basin are investigated using a combination of statistical analysis. Through the classification statistics of 84 rainfall events, it can be concluded that the rainfall characteristics of the Jingle sub-basin have changed significantly from 1980 to 2017, the proportion of type II and type III in 2000–2017 decreased by 8% and 2% respectively, while that of type I rainfall increased significantly. When precipitation > 25 mm, the surface runoff generated by rainfall increases by ~0.05 mm, and type I rainfall events will generate more runoff.

The land-use changes from 1971 to 2017 are ascertained using transition matrix analysis. From 1999 to 2017, the areas occupied by farmland, grassland, and forest decreased by 129.31 km^2, increased by 53.26 km^2 and 75.7 km^2, respectively. The increase of forest and grassland has obviously increased the vegetation coverage from 38% to 58% during the 2000–2017 periods. In order to study the influence of rainfall characteristics and vegetation increase on runoff of Jingle sub-basin, multiple nonlinear regression analysis was used to construct multivariate, nonlinear, model equations between runoff coefficient and rainfall intensity, vegetation coverage and other factors. When the V_c and API of the Jingle sub-basin maintain a stable value, the runoff coefficient of the shorter duration and higher intensity rainfall events (Type I) is greater than Type II and Type III. When V_c approaches 48%, the runoff coefficient decreased to the lowest, and the vegetation conditions have the greatest effect on reducing runoff.

The impacts of land-use and climate on runoff process are estimated using the *M-EIES* hydrological model and two scenarios. The land use effect decreased the water yield by 36.5% and the peak flow by 37%, and combined effect of climate and land use decrease in the two variables was 35.4% and 35.9% respectively. It can be concluded that for areas where land use has significantly improved, the impact of climate change on water yield is not obvious when the effect of land use change plays a dominant role. This study provides a deeper understanding of the interactions between rainfall characteristics, underlying surface conditions, and floods, and reveals the hydrological cycle mechanism in the areas where the underlying surface conditions of the middle reaches of the Yellow River have improved significantly.

Acknowledgements. This project was supported by Projects of National Natural Science Foundation of China (51979250); National key research priorities program of China (2016YFC040240203); National Key R&D Program of China (2019YFC1510703); National Natural Science Foundation of China (31700370); The National Key Research Priorities Program of China (2016YFC0402402); National Natural Science Foundation of China (51409116); Startup Research Fund of Zhengzhou University (1512323001); Institution of higher learning key scientific research project, Henan Province (16A570010); Foundation of drought climate science (IAM201705); China postdoctoral science foundation (2016M602255); Henan province postdoctoral science foundation; National Natural Science Foundation of China (91025015). We would like to thank LetPub (www.letpub.com) for providing linguistic assistance during the preparation of this manuscript.

REFERENCES

Asselman, N., Middelkoop, H., Van Dijk, P.M., 2003. The impact of changes in climate and land use on soil erosion, transport and deposition of suspended sediment in the River Rhine. Hydrol. Process., 17, 16, 3225–3244.

Bhark, E.W., Small, E.E., 2003. Association between plant canopies and the spatial patterns of infiltration in shrubland and grassland of the Chihuahuan Desert, New Mexico. Ecosystems, 6, 2, 185–196.

Chen, L., Sela, S., Svoray, T., 2013. The role of soil-surface sealing, microtopography, and vegetation patches in rainfall-runoff processes in semiarid areas. Water Resour. Res., 49, 9, 5585–5599.

Chen, X.F., Parajka, J., Széles, B., et al., 2020. Controls on event runoff coefficients and recession coefficients for different runoff generation mechanisms identified by three regression methods. J. Hydrol. Hydromech., 68, 2, 155−169.

Cuevas, J.G., Arumí, J.L., Dörner, J., 2019. Times of response of stream discharge as a function of rainfall duration in a southern Chilean watershed. J. Hydrol. Hydromech., 67, 2, 143−153.

Du, J.K., Qian, L., Rui, H.Y., et al., 2012. Assessing the effects of urbanization on annual runoff and flood events using an integrated hydrological modeling system for Qinhuai River basin, China. Journal of Hydrology, 465, 127–139.

Duan, Q.Y., Sorooshian, S., Gupta, V.K., 1992. Effective and efficient global optimization for conceptual rainfall-runoff models. Water Resour. Res., 28, 1015–1031.

Feng, X.M., Su, C.H., Liu, Y., et al., 2012. Regional effects of vegetation restoration on water yield across the Loess Plateau, China. Hydrol. Earth Syst. Sci., 16, 8, 2617–2628.

Gao, P., Mu, X.M., Wang, F., Li, R., 2011. Changes in streamflow and sediment dischargeand the response to human activities in the middle reaches of the Yellow River. Hydrol. Earth Syst. Sci., 15, 1, 1–10.

Gao, Y.Q., Chen, J.H., Luo, H., Wang, H.Z., 2020. Prediction of hydrological responses to land use change. Sci. Total Environ., 708, 134–142.

Hu, C., Li, S., Zhang, W., Chen, X., Wang, J., 2016. Establishing and testing runoff model based on runoff coefficient. J. China Hydrol., 36, 8–13.

Hu, C.H., Zhang, L., Jian, S.Q., et al., 2020. Response of LUCC on runoff generation process in Middle Yellow River basin: The Gushanchuan basin. Water, 12, 2–14.

Huff, F.A., 1967. Time distribution of rainfall in heavy storms. Water Resour. Res., 3, 4, 1007−1019.

Jeffrey, A.N., Eyal, A., 2003. High temporal resolution of extreme rainfall rate variability and the acoustic classification of rainfall. Journal of Geophysical Research: Atmospheres, 108, D8, Article Number: 8378.

Kong, D., et al., 2016. Impact assessment of climate change and human activities on net runoff in the Yellow River Basin from 1951 to 2012. Ecological Engineering. 91, 566–573.

Lewis, C.D., 1982. Industrial and Business Forecasting Methods: A Practical Guide to Exponential Smoothing and Curve Fitting. Butterworth Scientific, London.

Li, E.H., Mu, X.M., Zhao, G.J., Gao, P., Shao, H.B., 2014. Variation of runoff and precipitation in the Hekou-Longmen Region of the Yellow River based on elasticity analysis. Sci. World J., Article Number: 929858. https://doi.org/10.1155/2014/929858

Liu, J., Luo, M., Liu, T., et al., 2017. Local climate change and the impacts on hydrological processes in an Arid Alpine catchment in Karakoram. Water, 9, 5, Article Number: 344.

Liu, T., Huang, H.Q., Shao, M.A., et al., 2020. Integrated assessment of climate and human contributions to variation in streamflow in the Ten Great Gullies Basin of the Upper Yellow River, China. J. Hydrol. Hydromech., 68, 3, 249−259.

Ludwig, J.A., Wilcox, B.P., Breshears, D.D., et al., 2005. Vegetation patches and runoff-erosion as interacting ecohydrological processes in semiarid landscapes. Ecology, 86, 288–297.

Minea, G., Ioana-Toroimac, G., Moroşanu, G., 2019. The dominant runoff processes on grassland hillslopes within different land uses of Romania – an experimental study. J. Hydrol. Hydromech., 67, 4, 297−304.

Mu, W.B., Yu, F.L., Li, C.Z., et al., 2015. Effects of rainfall intensity and slope gradient on runoff and soil moisture content on different growing stages of spring maize. Water, 7, 6, Article Number: 2990.

Nau, R., 2017. Statistical Forecasting: Notes on Regression and Time Series Analysis. https://people.duke.edu/~rnau/compare.htm (Accessed 19th Oct 2017).

Ou, Y., Liu, L., Ye, S.Y., Liu, J.P., et al., 2018. Quantitative assessment of surface runoff and base flow response to multiple factors in Pengchongjian small watershed. Forests, 9, 9, Article Number: 553.

Oudin, L., Salavati, B., Saadi, M., 2018. Hydrological impacts of urbanization at the catchment scale. Journal of Hydrology, 559, 774–786.

Ran, D.C., Zuo, Z.G., Wu, Y.H., Li, X.M., Li, Z.H., 2012. Variation of Streamflow and Sediment in Response to Human Activities in the Middle Reaches of the Yellow River. Science Press, Beijing, China.

Walhin, J.F., 2000. Recursive formulae for some bivariate counting distributions obtained by the trivariate reduction

method. ASTIN Bulletin, 30, 1, 141–155.
Wang, S.Y., Huang, Y.J., Chen, Z.X., 2005. Remote sensing study of returning farmland to forest or grassland in the Yellow River Basin. J. Tsinghua Univ. Sci. Tech., 45, 306–309.
Wang, Y.H., Yu, P.T., Xiong, W., et al., 2008. Water yield reduction after afforestation and related process in the semi-arid Liupan Mountains, Northwest China. J. Am. Water Resour. Assoc., 44, 5, 1086–1097.
Wang, S.J., Li, L., Yan, M., 2013. The contributions of climate change and human activities to the runoff yield change in the middle Yellow River basin. Geogr. Res., 32, 3, 395–402. (In Chinese.)
Wang, S., Fu, B., Piao, S., Lü, Y., Ciais, P., Feng, X., Wang, Y., 2015. Reduced sediment transport in the Yellow River due to anthropogenic changes. Nat. Geosci., 9, 38–41.
Wang, D., Jian, S.Q., Hu, C.H., 2018. Impact of climate change and human activities on runoff in Fenhe River basin. Arid Land Geography, 41, 25–31.
Wang, X.J., Zhang, P.F., Liu, L.L., 2019. Effects of human activities on hydrological components in the Yiluo River basin in Middle Yellow River. Water, 11, 689.
Wen, Y.X., Hu, C.H., Jian, S.Q., 2020. Response of the parameters of excess infiltration and excess storage model to land use cover change. J. Hydrol. Hydromech., 68, 2, 99−110.
Wu, L.H., Wang, S.J., Bai, X.Y., 2017. Quantitative assessment of the impacts of climate change and human activities on runoff change in a typical karst watershed, SW China. Sci. Total Environ., 601, 1449–1465.
Xin, Z.B., Yu, X.X., 2009. Impact of vegetation restoration on hydrological processes in the middle reaches of the Yellow River, China. Forestry Studies in China, 11, 4, 209–218.
Yang, J., Lei, H.M., Yang, D.W., et al., 2017. Impact of vegetation dynamics on hydrological processes in a semi-arid basin by using a land surface-hydrology coupled model. Journal of Hydrology, 551, 116–131.
Yang, X., Sun, W., Li, P., Mu, X., Gao, P., Zhao, G., 2018. Reduced sediment transport in the Chinese Loess Plateau due to climate change and human activities. Sci. Total Environ., 642, 591–600.
Yang, C.X., Yao, W.Y., Xiao, P.Q., 2019a. Effects of vegetation cover structure on runoff and sediment yield and its regulation mechanism. Journal of Hydraulic Engineering, 50, 9, 1078–1085.
Yang, Y.B., Zhang, J.J., Li, L., et al., 2019b. Effects of rainfall process on runoff in small watersheds in the Loess Plateau of western Shanxi Province. Journal of Beijing Forestry University, 41, 3, 105–114.
Yin, S.Q., Wang, Y., Xie, Y., et al., 2014. Characteristics of intra-storm temporal pattern over China. Advances in Water Science, 25, 5, 617−623.
Yin, J., He, F., Xiong, Y., 2017. Effects of land use/land cover and climate changes on surface runoff in a semi-humid and semi-arid transition zone in northwest China. Hydrol. Earth Syst. Sci., 21, 1, 183–196.
Yue, X., Mu, X., Zhao, G., Shao, H., Gao, P., 2014. Dynamic changes of sediment load in the middle reaches of the Yellow River basin, China and implications for eco-restoration. Ecol. Eng., 73, 64–72.
Zhan, C.S., Jiang, S.S., Sun, F.B., 2014. Quantitative contribution of climate change and human activities to runoff changes in the Wei River basin, China. Hydrol. Earth Syst. Sci., 18, 3069–3077.
Zhao, R.J., 1992. The Xinanjiang model applied in China. Journal of Hydrology, 135, 371–381.
Zhao, G.J., Tian, P., Mu, X.M., et al., 2013a. Climate changes and their impacts on water resources in semiarid regions: a case study of the Wei River basin, China. Hydrological Processes, 27, 3852–3863.
Zhao, G., Mu, X., Wen, Z., Wang, F., Gao, P., 2013b. Soil erosion, conservation, and eco-environment changes in the loess plateau of China. Land Degrad. Dev., 24, 499–510.
Zope, P.E., Eldho, T.I., Jothiprakash, V., 2016. Impacts of land use–land cover change and urbanization on flooding: A case study of Oshiwara River Basin in Mumbai, India. Catena, 145, 142–154.
Zuo, D.P., Xu, Z.X., Yao, W.Y., et al., 2016. Assessing the effects of changes in land use and climate on runoff and sediment yields from a watershed in the Loess Plateau of China. Sci. Total Environ., 544, 238–250.

Received 23 October 2020
Accepted 23 November 2020